HHS Public Access

Author manuscript

Antioxid Redox Signal. Author manuscript; available in PMC 2015 July 16.

Published in final edited form as:

Antioxid Redox Signal. 2003 October ; 5(5): 507–516. doi:10.1089/152308603770310158.

Iron Accumulation During Cellular Senescence in Human Fibroblasts *In Vitro*

DAVID W. KILLILEA[1,2], **HANI ATAMNA**[1], **CHARLES LIAO**[2], and **BRUCE N. AMES**[1,2]

[1]Children's Hospital Oakland Research Institute, Oakland, CA 94609

[2]Molecular and Cellular Biology, University of California at Berkeley, Berkeley, CA 94720

Abstract

Iron accumulates as a function of age in several tissues *in vivo* and is associated with the pathology of numerous age-related diseases. The molecular basis of this change may be due to a loss of iron homeostasis at the cellular level. Therefore, changes in iron content in primary human fibroblast cells (IMR-90) were studied *in vitro* as a model of cellular senescence. Total iron content increased exponentially during cellular senescence, resulting in 10-fold higher levels of iron compared with young cells. Low-dose hydrogen peroxide (H_2O_2) induced early senescence in IMR-90s and concomitantly accelerated iron accumulation. Furthermore, senescence-related and H_2O_2-stimulated iron accumulation was attenuated by *N-tert*-butylhydroxylamine (NtBHA), a mitochondrial antioxidant that delays senescence *in vitro.* However, SV40-transformed, immortalized IMR-90s showed no time-dependent changes in metal content in culture or when treated with H_2O_2 and/or NtBHA. These data indicate that iron accumulation occurs during normal cellular senescence *in vitro.* This accumulation of iron may contribute to the increased oxidative stress and cellular dysfunction seen in senescent cells.

INTRODUCTION

Cellular senescence is the process by which most normal cells progressively lose replicative capacity and become refractory to further proliferation. Senescent cells undergo substantial phenotypical changes that include altered volume, morphology, gene expression, and metabolism (12, 16). Senescent cells are also observed to have higher levels of oxidative stress than younger cells; oxidants are increasingly produced as mitochondrial and lysosomal functions decay, antioxidant defenses decline, and repair mechanisms falter (8). Oxidative stress is also mediated by redox-active metals, of which iron is the most abundant. Iron is required for cellular function, but iron may also catalyze formation of oxidants that can damage cellular macromolecules (25). Normally, cellular iron homeostasis is well balanced to maintain cellular requirements while minimizing participation in pro-oxidative Fenton chemistry. However, oxidants, *e.g.*, superoxide radical and hydrogen peroxide (H_2O_2) from dysfunctional mitochondria, can disrupt iron homeostasis to increase labile iron

Address reprint requests to: Dr. Bruce N. Ames, Nutritional Genomics Center, Children's Hospital Oakland Research Institute, 5700 Martin Luther King, Jr. Way, Oakland, CA 94609, BAmes@chori.org.

and lead to further oxidative stress (11, 33). Thus, oxidant-mediated changes in iron homeostasis may initiate a vicious cycle that ultimately results in cellular or tissue injury.

Iron homeostasis appears to become corrupted with age. Aging-related increases in body iron stores have been associated with normal aging (15, 24, 49). Additionally, iron accumulation has also been seen in aging-related disorders, including Alzheimer's disease (37, 40), Parkinson's disease (26, 48, 50), type 2 diabetes (19, 36), and cardiovascular disease (39, 43). Loss of iron homeostasis at the cellular level may be the underlying basis for these changes in tissue iron (6, 45).

In this study, we investigated the effects of cellular senescence on intracellular iron content in primary human cells *in vitro.* Changes in iron content were also determined in cultures treated with *N-tert*-butylhydroxylamine (NtBHA), an antioxidant that is protective against mitochondrial dysfunction and delays cellular senescence (3), and H_2O_2, an oxidant that at low doses accelerates cellular senescence (3, 47). These models of accelerated and decelerated senescence resulted in parallel changes of intracellular iron content in primary fibroblasts. However, no correlation between proliferation and iron content existed in immortalized fibroblasts. This indicates a relationship between cellular senescence and iron accumulation. Thus, models of *in vitro* senescence may prove useful to study iron homeostasis *in vivo.* Given the propensity of iron to exacerbate oxidative stress and the strong association of oxidative stress with cellular senescence, elucidating how iron homeostasis changes at the cellular level will be critical to understand the role of iron in age-related disease.

MATERIALS AND METHODS

Materials

All cell culture reagents were purchased from InVitrogen Inc. (Carlsbad, CA, U.S.A.), except for fetal bovine serum (FBS; Hyclone, Logan, UT, U.S.A.) and endothelial cell growth supplement (ECGS; Sigma–Aldrich, St. Louis, MO, U.S.A.). Chelex-100 resin was purchased from Bio-Rad (Hercules, CA, U.S.A.). OmniTrace 70% nitric acid and trace metal-free glassware were purchased from VWR (West Chester, PA, U.S.A.). National Institute of Standards and Technology (NIST) traceable powdered bovine liver tissue (sample 1577b) was a generous gift from Paul Brooks (Berkeley, CA, U.S.A.). NtBHA, *O-tert*-butylhydroxylamine (OtBHA), diethylenetriamine pentaacetic acid (DTPA), and all other reagents were purchased from Sigma–Aldrich. Metal-stripped water was prepared using distilled water mixed with Chelex-100 resin (5% wt/vol) for 12 h at 200 rpm and then filtered; water was routinely checked for metal contamination.

Cell culture

Primary (IMR-90) and simian virus 40 (SV40)-transformed (SV-IMR-90) human diploid lung fibroblasts were both purchased from the Coriell Institute of Medical Research (Camden, NJ, U.S.A.). IMR-90s were obtained at 11 population doublings (PD). Postcrisis SV-IMR-90s, originating from the same pool as primary IMR-90s, were obtained at ~120 PDs. SV-IMR-90s were 100% T-antigen positive, but grew adherent and exhibited contact

inhibition. Both fibroblast populations were cultivated in Dulbecco's modified Eagle's medium supplemented with 10% FBS, 100 units/ml penicillin, and 100 μg/ml streptomycin. Human umbilical vein endothelial cells (HUVECs) were purchased from American Type Culture Collection (Manassas, VA, U.S.A.) and obtained at 36 PDs. HUVECs were cultivated in F-12K nutrient mixture supplemented with 15% FBS, 0.1 mg/ml heparin, 30 μg/ml ECGS, 100 units/ml penicillin, and 100 μg/ml streptomycin. Adherent cells were detached using 0.05% trypsin and 0.5 m*M* EDTA for 5 min at 37°C. Replicative age was determined in PD calculated as $\log_2(D/D_o)$ where D and D_o are density at time of harvest and seeding, respectively (3).

For chronic treatment with NtBHA or OtBHA, cultures were passaged weekly, allowed 1 day to reattach and resume normal growth, and then treated with 10 μ*M* or 100 μ*M* NtBHA or 100 μ*M* OtBHA. For repeated treatment with low doses of H_2O_2, cultures were passaged weekly, allowed 1 day to reattach and resume normal growth, and then treated with 10 μ*M* or 20 μ*M* H_2O_2 added directly to culture media. For treatment with H_2O_2 and NtBHA, cultures were passaged weekly, allowed 1 day to reattach and resume normal growth, and treated with 10 μ*M* or 20 μ*M* H_2O_2. Then NtBHA was added 1 day after H_2O_2 treatment to prevent the possibility of NtBHA directly blocking H_2O_2 action within the cell as an antioxidant. These treatments did not cause any significant change in cell viability as assessed by vital dye exclusion and tetrazolium dye reduction assays (data not shown).

Cell counting and volume analysis

Adherent cells were detached and then processed to single-cell suspension using repeated pipeting in Hanks' balanced salt solution. Cells were counted on a Z2 Coulter Counter equipped with multisizing capabilities (Beckman Coulter, Fullerton, CA, U.S.A.). Diameter ranges were 13–25 μm for IMR-90s, 11–23 μm for SV-IMR-90s, and 11–22 μm for HUVECs. Mean cell volume was determined using native software.

Inductively coupled plasma optical-emission spectroscopy (ICP)

Cells were harvested, counted in triplicate, and processed for elemental analysis as described (5, 28). Routinely, three aliquots of 5×10^6 cells were prepared in sterile polystyrene tubes and dehydrated at 60°C for 12–16 h. The cellular material was then digested in 0.5 ml of OmniTrace 70% nitric acid in a shaking incubator (200 rpm) at 37°C for 12–16 h. NIST-traceable indium, used as an internal standard, was added to each tube to 1 μg/ml. The cellular digests were then diluted in metal-stripped water, clarified by centrifugation for 10 min at 3,000 *g*, and processed via ICP (IRIS 5900, Thermo Elemental, Franklin, MA, U.S.A.). ICP operating conditions included 1,150 W of RF power, 0.5 L/min argon carrier gas, and 29 psi in a Burgener nebulizer. The ICP was calibrated using NIST-traceable elemental standards and verified using a NIST-traceable bovine liver tissue standard. All standards and samples were run in a matrix of 8% nitric acid. NIST-traceable scandium standard was added in line at 1 μg/ml for external (flow) control. During each run, the content of each element was determined using an average value from multiple wavelengths when available.

Statistical methods

Graphing, regression, and statistical analysis were performed using Prism 3.0 (GraphPad, San Diego, CA, U.S.A.) software. Significance was accepted as $p < 0.05$.

RESULTS

Iron accumulation in cultured IMR-90s

Primary human fibroblasts (IMR-90s) were cultured until senescent at ~50–55 PD (Fig. 1A). Senescence-dependent increases in cellular volume and total cellular protein were observed; volume increased 1.2-fold (3,419.9 ± 107.9 fl for young cells and 3,984.9 ± 223.1 fl for old cells; $n = 3$, $p < 0.05$ using Mann–Whitney test), and protein increased on average 1.8-fold (0.025 ± 0.005 μg/10^5 for young cells and 0.046 ± 0.004 μg/10^5 for old cells; $n = 3$, $p < 0.05$ using Student's *t* test). At various PDs, IMR-90s were analyzed for metal content and normalized to cell number. Total intracellular iron content increased exponentially with increasing PD to ~10-fold, with doubling of iron content at approximately every 9 PDs (Fig. 1B). Senescence-associated increases in cellular volume or total protein did not contribute substantially to increased iron content because iron still accumulated four- to fivefold when normalized to either volume or protein levels. To rule out contamination from extracellular iron bound to phospholipids on the cell surface, duplicate cell pellets were washed with 5 m*M* DTPA, a strong but cell-impermeant metal chelator. No difference in iron content was observed with or without DTPA, indicating that the observed values reflect only the total intracellular iron content (unpublished observations).

The intracellular content of magnesium, potassium, manganese, and zinc also increased by two- to fivefold during the population life span, although less than the change in intracellular iron (Table 1). Moreover, the time for the levels of these metals to double took 50–300% longer than that for iron, suggesting that iron accumulation precedes the changes in these other metals.

Iron accumulation in cultured HUVECs

A senescence-associated increase in iron content was also observed in HUVECs. HUVECs demonstrated growth kinetics similar to IMR-90s, becoming senescent at ~55–60 PD (data not shown). Total intracellular iron content increased exponentially with increasing PD to ~50-fold, with doubling of iron content at approximately every 5 PDs (Table 1). A senescence-dependent increase in magnesium, potassium, manganese, and zinc was also observed, but to a lesser degree. The accumulation of these metals was more delayed than that of iron, suggesting that iron content is the first to change during cellular senescence, as with IMR-90 cultures.

No change in iron content in cultured SV-IMR-90s

Iron content in immortalized, SV-IMR-90s, established from the same genetic stock of primary IMR-90s, showed no loss of replicative capacity over time (Fig. 1C). No change in total intracellular iron content was observed in SV-IMR-90s over 5 months of cultivation under conditions identical to those for primary IMR-90s (Fig. 1D). Additionally, there was

no effect of proliferation on the intracellular content of magnesium, potassium, manganese, and zinc (Table 1).

NtBHA delays senescence-associated iron accumulation in IMR-90s

Weekly NtBHA treatment of IMR-90s delayed senescence in a dose-dependent manner (Fig. 2A). Concomitantly, NtBHA caused a dose-dependent delay of senescence-associated accumulation of iron (Fig. 2B). Iron accumulation was suppressed by >70% with weekly doses of 100 μ*M* NtBHA by the end of the normal cellular life span. NtBHA also delayed senescence-associated increases in magnesium and zinc content (Table 2). IMR-90s similarly treated with OtBHA, an isomer of NtBHA without antisenescent activity (3), did not affect senescence-associated iron accumulation (Table 2).

SV-IMR-90s were similarly cultured with NtBHA or OtBHA under the same conditions as IMR-90s and evaluated for changes in proliferation and iron content. Neither NtBHA nor OtBHA affected SV-IMR-90 growth rate (Fig. 2C) or iron content (Fig. 2D). Additionally, neither NtBHA nor OtBHA treatment significantly affected intracellular levels of magnesium and zinc because slopes of fit curves were not statistically different from control (Table 2).

Oxidative stress accelerates senescence-associated iron accumulation in IMR-90s

Repeated exposure to low-dose H_2O_2 accelerated senescence in IMR-90s in a dose-dependent manner (Fig. 3A). H_2O_2-induced early senescence correlated with a dose-dependent increase in iron content (Fig. 3B). However, H_2O_2 treatment did not accelerate senescence-related increases in magnesium and zinc content, although these metals still increased over time (Table 3).

Previous work demonstrated that NtBHA protected against H_2O_2-induced early senescence (3). In order to gain more insight into the activity of NtBHA, we tested its effect on H_2O_2-accelerated senescence and iron accumulation. Even when added 24 h after H_2O_2, NtBHA reversed the loss of PD induced by H_2O_2 (Fig. 3A) and prevented H_2O_2-induced iron accumulation (Fig. 3B). No attenuation of growth or iron accumulation was seen when NtBHA was replaced with OtBHA in all cases. NtBHA also blocked senescence-related increases in magnesium and zinc even after H_2O_2 treatment (Table 3).

The effects of oxidant stress on proliferation and iron accumulation were also tested with SV-IMR-90s under the same conditions as IMR-90s. H_2O_2 treatment dose-dependently slowed SV-IMR-90 proliferation; the slope of the 10 μ*M* H_2O_2 line was <1% lower and the slope of the 20 μ*M* H_2O_2 line was <15% lower than the slope of the control line. However, H_2O_2 treatment did not induce replicative block or senescent-like phenotype as in IMR-90s (Fig. 3C). Moreover, H_2O_2 did not alter intracellular iron content in SV-IMR-90s (Fig. 3D). NtBHA treatment provided no protection against H_2O_2-mediated decrease in proliferation (Fig. 3C) and no effect on intracellular iron levels (Fig. 3D). Additionally, neither H_2O_2 alone nor in combination with NtBHA significantly affected intracellular levels of magnesium or zinc, because slopes of curves from treated conditions were not statistically

different from control (Table 3). Furthermore, no effects on proliferation or iron accumulation were seen when NtBHA was replaced with OtBHA in all cases.

DISCUSSION

Intracellular iron levels increased exponentially in cultured primary human fibroblasts and in umbilical vein endothelial cells as a function of cellular senescence (Fig. 1). Intracellular magnesium, potassium, manganese, and zinc also increased with age, but to a lesser degree and later in life span than iron (Table 1). It is difficult to explain these observations with a single hypothesis, as these metals have little direct metabolic overlap. Increased cellular volume and protein content might have some effect on metal homeostasis, but are not likely to be major factors because the change in iron and other metals content exceeded the change in volume and protein levels. Therefore, cellular uptake or excretion of iron and other metals seems to be specifically affected by cellular changes during senescence. The physiological changes during cellular senescence are extensive, so it is conceivable that altered homeostasis of metals is a part of an overall metabolic disruption encountered during senescence. Some studies have reported altered metal homeostasis in human cells during cellular senescence (29, 42). Because iron accumulates at both a greater rate and capacity than the other metals measured, and due to the relevance of iron to aging-related diseases, we focused on the changes in iron content during cellular senescence.

Normal cellular senescence seems to be associated with accumulation of iron, because there was no change in iron content in SV40-transformed, immortalized IMR-90s after 5 months in culture (Fig. 1). SV40 transformation results in the inactivation of p53 and the retinoblastoma protein (pRb) (27), but also may involve inhibition of the transcriptional activators p300 and CREB-binding protein (1, 13), suggesting that the mechanisms responsible for altered iron content occur subsequent to cell-cycle checkpoints and/or expression changes that are central to producing the senescence phenotype. Moreover, as senescence mechanisms must be intact to observe increases in intracellular iron, iron accumulation is likely not an endogenous trigger for cellular senescence, but a consequence of senescence-mediated changes in cell physiology.

Additional support for a relationship between iron accumulation and cellular senescence came from experiments using NtBHA. NtBHA was previously shown to delay senescence *in vitro,* which may be due to a protective effect against senescence-related increases in oxidative stress and mitochondrial decay (3, 4). The antisenescence effect of NtBHA was utilized to assess the role of iron in cellular senescence. NtBHA-treated IMR-90s demonstrated delayed cellular senescence, which correlated with attenuated accumulation of iron in primary, but not immortalized IMR-90s (Fig. 2). Pretreatment of cells with NtBHA has been shown to block H_2O_2-accelerated senescence *in vitro* (3, 4). In this study, NtBHA attenuated H_2O_2-accelerated senescence and concomitant iron accumulation in primary, but not immortalized IMR-90s (Fig. 3). Interestingly, the protective effect of NtBHA was still seen even when added a full day after H_2O_2 treatment, indicating that NtBHA was able to actually reverse the damage caused by oxidant stress that promoted early senescence and cellular dysfunction.

The antisenescent mechanism of NtBHA is not known. Although this compound has antioxidant activity, numerous other antioxidants failed to delay cellular senescence (3, 34, 38). NtBHA also prevented iron accumulation in IMR-90s, but direct metal chelation is unlikely because NtBHA had no effect on the metal content in SV-IMR-90s. Furthermore, the known iron chelators desferrioxamine and salicylaldehyde isonicotinoyl hydrazone did not delay senescence when cells were treated at subtoxic concentrations, despite dose-dependent reduction in total iron content up to 50% of control (data not shown). Additionally, NtBHA delayed mitochondria dysfunction and oxidative stress during senescence (3, 4). Mitochondrial dysfunction, proposed to be an early event during aging and senescence (2, 23), is likely to play a role in senescence-related changes in iron homeostasis for several reasons. Mitochondria are the location for biosynthesis of heme and iron-sulfur clusters, which change with age as discussed below (6). Also, both experimental iron overload and deficiency can cause mitochondrial dysfunction (9, 46). Moreover, several systems with identified mitochondrial abnormalities, such as mutations in mitochondrial frataxin (7) or mitochondrial DNA-depletion (ρ-0 cells) (21), resulted in mitochondrial iron overload. Now we report that NtBHA, known to protect mitochondrial function during oxidant stress and senescence (3, 4), attenuated iron accumulation during senescence. We are currently defining the physiological targets of NtBHA with major emphasis on mitochondrial pathways.

Further support for the possible relationship between iron accumulation and cellular senescence came from experiments using H_2O_2. Repeated exposure to low-dose H_2O_2 may mimic the oxidative stress that occurs during cellular senescence in terms of level and type of oxidants (3, 47). This treatment caused early senescence in IMR-90s, with a concomitant increase in iron content (Fig. 3). When immortalized IMR-90s were treated with H_2O_2 under similar conditions, there was no correlation between proliferation and iron content, further demonstrating the association of iron accumulation with cellular aging.

Although the effects of H_2O_2 on senescence have been studied (14, 20), the mechanism is still not completely defined. However, oxidant stress is known to alter intracellular iron homeostasis (11, 33). H_2O_2-mediated iron accumulation may involve activation of the iron-response proteins (IRPs), IRP-1 and IRP-2. IRPs coordinately regulate iron uptake, storage, and metabolism to match iron availability with cellular need (18). Oxidants can collapse the iron-sulfur cluster in IRP-1 causing activation of the protein (35), although this is controversial because oxidation of specific thiols can inactivate IRP-1 (10). Oxidative stress may also indirectly stabilize IRP-2, as IRP-2 is regulated mainly by proteosomal degradation machinery that is inhibited by direct oxidation and oxidatively crosslinked proteins (18, 22). Additionally, ferrochetalase, the terminal enzyme involved in heme synthesis, may be inactivated by oxidative stress (44), inducing heme deficiency in cells. Heme deficiency leads to accumulation of iron in human fibroblasts and brain cell lines (5). Heme deficiency also may affect a diverse number of cellular processes, as indicated by the newly emerging roles for heme in cell signaling and gene expression regulations (6); the effects of these processes on iron accumulation remain to be identified.

The biological significance of senescence-related increases in intracellular iron content is not understood. However, we propose that senescence-related oxidative stress may induce

an “iron-starved” phenotype in the cells via *uncoupling* iron sensing and iron uptake mechanisms. The uncoupling of iron homeostasis with oxidants has been demonstrated in other systems; for example, IRP activity dose-dependently increased in murine fibroblasts during H_2O_2 treatment even in the presence of an excess of exogenous iron (35). It is plausible that increasing oxidative stress associated with senescence might elicit a similar response in human cells, leading to intracellular iron accumulation. The data from cultures treated with NtBHA and H_2O_2 support this perspective. Thus, iron accumulation may simply be a negative consequence of increased oxidant production during senescence that contributes to the overall level of oxidative stress within the cell. Support for this idea comes from work in other systems where iron accumulation was associated with decreased life span and iron chelation provides life-span extension (30, 31, 41). On the other hand, intracellular iron accumulation might have positive aspects *in vivo.* Increased iron uptake may reduce labile iron in tissues. Then incorporation of iron into ferritin, shown to be increased under conditions of oxidative stress *in vitro,* could protect against further oxidant-mediated toxicity (11). Increased intracellular iron availability may also protect against oxidative damage by increasing heme and iron-sulfur cluster cofactor levels for critical proteins, including ribonucleotide reductase to produce more nucleotides for DNA repair, catalase to detoxify H_2O_2, or electron transport chain subunits for cellular energy production (5, 6).

In sum, these data strongly support the hypothesis that iron homeostasis is altered during cellular senescence. To our knowledge, this is the first report demonstrating senescence-related iron accumulation in cultured primary human cells. Understanding the detailed mechanisms that drive this accumulation of iron may lead to new insights into the processes involved in cellular senescence. Understanding the functional consequences of this iron accumulation may lead to new opportunities for intervention against age-related dysfunction, as therapeutic approaches for altering iron levels *in vivo* are in common clinical use. In fact, iron chelation therapy has recently been identified as a promising new therapy for Alzheimer’s disease (17, 32). Perhaps iron overload with age, especially in age-related disease, has its roots in senescence-related iron accumulation at the cellular level.

Acknowledgments

The authors thank Wafa Atamna, Paul Brooks, and Carla Schultz for technical support. This work was supported in part by NIA Training Grant (5 T32 AG00266–02) for D.W.K. and Ellison Medical Foundation Grant (SS-OA22–99) for B.N.A.

ABBREVIATIONS

DTPA	diethylenetriamine pentaacetic acid
ECGS	endothelial cell growth supplement
FBS	fetal bovine serum
H_2O_2	hydrogen peroxide
HUVEC	human umbilical vein endothelial cell

ICP	inductively coupled plasma optical-emission spectroscopy
IRP	iron response protein
NIST	National Institute of Standards and Technology
NtBHA	*N-tert*-butylhydroxylamine
OtBHA	*O-tert*-butylhydroxylamine
PD	population doubling
SV40	simian virus 40
SV-IMR-90	SV40-transformed IMR-90

References

1. Ali SH, DeCaprio JA. Cellular transformation by SV40 large T antigen: interaction with host proteins. Semin Cancer Biol. 2001; 11:15–23. [PubMed: 11243895]
2. Ames BN, Shigenaga MK, Hagen TM. Mitochondrial decay in aging. Biochim Biophys Acta. 1995; 1271:165–170. [PubMed: 7599204]
3. Atamna H, Paler-Martinez A, Ames BN. *N-t-Butyl* hydroxylamine, a hydrolysis product of alpha-phenyl-*N-t*-butyl nitrone, is more potent in delaying senescence in human lung fibroblasts. J Biol Chem. 2000; 275:6741–6748. [PubMed: 10702229]
4. Atamna H, Robinson C, Ingersoll R, Elliott H, Ames BN. *N-t*-Butyl hydroxylamine is an antioxidant that reverses age-related changes in mitochondria in vivo and in vitro. FASEB J. 2001; 15:2196–2204. [PubMed: 11641246]
5. Atamna H, Killilea DW, Killilea AN, Ames BN. Heme deficiency may be a factor in the mitochondrial and neuronal decay of aging. Proc Natl Acad Sci U S A. 2002; 99:14807–14812. [PubMed: 12417755]
6. Atamna H, Walter PB, Ames BN. The role of heme and iron-sulfur clusters in mitochondrial biogenesis, maintenance, and decay with age. Arch Biochem Biophys. 2002; 397:345–353. [PubMed: 11795893]
7. Babcock M, de Silva D, Oaks R, Davis-Kaplan S, Jiralerspong S, Montermini L, Pandolfo M, Kaplan J. Regulation of mitochondrial iron accumulation by Yfh1p, a putative homolog of frataxin. Science. 1997; 276:1709–1712. [PubMed: 9180083]
8. Beckman KB, Ames BN. The free radical theory of aging matures. Physiol Rev. 1998; 78:547–581. [PubMed: 9562038]
9. Britton RS, Leicester KL, Bacon BR. Iron toxicity and chelation therapy. Int J Hematol. 2002; 76:219–228. [PubMed: 12416732]
10. Cairo G, Pietrangelo A. Iron regulatory proteins in pathobiology. Biochem J. 2000; 352(Pt 2):241–250. [PubMed: 11085915]
11. Caltagirone A, Weiss G, Pantopoulos K. Modulation of cellular iron metabolism by hydrogen peroxide. Effects of H_2O_2 on the expression and function of iron-responsive element-containing mRNAs in B6 fibroblasts. J Biol Chem. 2001; 276:19738–19745. [PubMed: 11264285]
12. Campisi J. Cellular senescence and apoptosis: how cellular responses might influence aging phenotypes. Exp Gerontol. 2003; 38:5–11. [PubMed: 12543256]
13. Chen H, Campisi J, Padmanabhan R. SV40 large T antigen transactivates the human cdc2 promoter by inducing a CCAAT box binding factor. J Biol Chem. 1996; 271:13959–13967. [PubMed: 8662914]
14. Chen QM, Bartholomew JC, Campisi J, Acosta M, Reagan JD, Ames BN. Molecular analysis of H_2O_2-induced senescent-like growth arrest in normal human fibroblasts: p53 and Rb control G1 arrest but not cell replication. Biochem J. 1998; 332 (Pt 1):43–50. [PubMed: 9576849]

15. Connor JR, Snyder BS, Beard JL, Fine RE, Mufson EJ. Regional distribution of iron and iron-regulatory proteins in the brain in aging and Alzheimer's disease. J Neurosci Res. 1992; 31:327–335. [PubMed: 1573683]
16. Cristofalo VJ, Pignolo RJ. Molecular markers of senescence in fibroblast-like cultures. Exp Gerontol. 1996; 31:111–123. [PubMed: 8706781]
17. Cuajungco MP, Faget KY, Huang X, Tanzi RE, Bush AI. Metal chelation as a potential therapy for Alzheimer's disease. Ann N Y Acad Sci. 2000; 920:292–304. [PubMed: 11193167]
18. Eisenstein RS. Iron regulatory proteins and the molecular control of mammalian iron metabolism. Annu Rev Nutr. 2000; 20:627–662. [PubMed: 10940348]
19. Fernandez-Real JM, Lopez-Bermejo A, Ricart W. Cross-talk between iron metabolism and diabetes. Diabetes. 2002; 51:2348–2354. [PubMed: 12145144]
20. Frippiat C, Dewelle J, Remacle J, Toussaint O. Signal transduction in H_2O_2-induced senescence-like phenotype in human diploid fibroblasts. Free Radic Biol Med. 2002; 33:1334–1346. [PubMed: 12419465]
21. Fukuyama R, Nakayama A, Nakase T, Toba H, Mukainaka T, Sakaguchi H, Saiwaki T, Sakurai H, Wada M, Fushiki S. A newly established neuronal rho-0 cell line highly susceptible to oxidative stress accumulates iron and other metals. Relevance to the origin of metal ion deposits in brains with neurodegenerative disorders. J Biol Chem. 2002; 277:41455–41462. [PubMed: 12194972]
22. Grune T. Oxidative stress, aging and the proteasomal system. Biogerontology. 2000; 1:31–40. [PubMed: 11707918]
23. Hagen TM, Yowe DL, Bartholomew JC, Wehr CM, Do KL, Park JY, Ames BN. Mitochondrial decay in hepatocytes from old rats: membrane potential declines, heterogeneity and oxidants increase. Proc Natl Acad Sci U S A. 1997; 94:3064–3069. [PubMed: 9096346]
24. Hallgren B, Sourander P. The effect of age on the nonhaemin iron in the human brain. J Neurochem. 1958; 3:41–51. [PubMed: 13611557]
25. Halliwell B. Free radicals and metal ions in health and disease. Proc Nutr Soc. 1987; 46:13–26. [PubMed: 3575319]
26. Hirsch EC, Brandel JP, Galle P, Javoy-Agid F, Agid Y. Iron and aluminum increase in the substantia nigra of patients with Parkinson's disease: an X-ray microanalysis. J Neurochem. 1991; 56:446–451. [PubMed: 1988548]
27. Itahana K, Dimri G, Campisi J. Regulation of cellular senescence by p53. Eur J Biochem. 2001; 268:2784–2791. [PubMed: 11358493]
28. Liu J, Killilea DW, Ames BN. Age-associated mitochondrial oxidative decay: improvement of carnitine acetyltransferase substrate-binding affinity and activity in brain by feeding old rats acetyl-L-carnitine and/or *R*-alpha-lipoic acid. Proc Natl Acad Sci U S A. 2002; 99:1876–1881. [PubMed: 11854488]
29. Liu S, Thweatt R, Lumpkin CK Jr, Goldstein S. Suppression of calcium-dependent membrane currents in human fibroblasts by replicative senescence and forced expression of a gene sequence encoding a putative calcium-binding protein. Proc Natl Acad Sci U S A. 1994; 91:2186–2190. [PubMed: 8134370]
30. Massie HR, Aiello VR, Williams TR. Iron accumulation during development and ageing of *Drosophila*. Mech Ageing Dev. 1985; 29:215–220. [PubMed: 3919221]
31. Massie HR, Aiello VR, Williams TR. Inhibition of iron absorption prolongs the life span of *Drosophila*. Mech Ageing Dev. 1993; 67:227–237. [PubMed: 8326745]
32. Maynard CJ, Cappai R, Volitakis I, Cherny RA, White AR, Beyreuther K, Masters CL, Bush AI, Li QX. Overexpression of Alzheimer's disease amyloid-beta opposes the age-dependent elevations of brain copper and iron. J Biol Chem. 2002; 277:44670–44676. [PubMed: 12215434]
33. Nunez-Millacura C, Tapia V, Munoz P, Maccioni RB, Nunez MT. An oxidative stress-mediated positive-feedback iron uptake loop in neuronal cells. J Neurochem. 2002; 82:240–248. [PubMed: 12124425]
34. Packer L, Smith JR. Extension of the lifespan of cultured normal human diploid cells by vitamin E: a reevaluation. Proc Natl Acad Sci U S A. 1977; 74:1640–1641. [PubMed: 266202]
35. Pantopoulos K, Hentze MW. Rapid responses to oxidative stress mediated by iron regulatory protein. EMBO J. 1995; 14:2917–2924. [PubMed: 7796817]

36. Perez de Nanclares G, Castano L, Gaztambide S, Bilbao JR, Pi J, Gonzalez ML, Vazquez JA. Excess iron storage in patients with type 2 diabetes unrelated to primary hemochromatosis. N Engl J Med. 2000; 343:890–891. [PubMed: 11001697]
37. Perry G, Taddeo MA, Petersen RB, Castellani RJ, Harris PL, Siedlak SL, Cash AD, Liu Q, Nunomura A, Atwood CS, Smith MA. Adventiously-bound redox active iron and copper are at the center of oxidative damage in Alzheimer disease. Biometals. 2003; 16:77–81. [PubMed: 12572666]
38. Poot M. Oxidants and antioxidants in proliferative senescence. Mutat Res. 1991; 256:177–189. [PubMed: 1722009]
39. Salonen JT, Nyyssonen K, Korpela H, Tuomilehto J, Seppanen R, Salonen R. High stored iron levels are associated with excess risk of myocardial infarction in eastern Finnish men. Circulation. 1992; 86:803–811. [PubMed: 1516192]
40. Smith MA, Harris PL, Sayre LM, Perry G. Iron accumulation in Alzheimer disease is a source of redox-generated free radicals. Proc Natl Acad Sci U S A. 1997; 94:9866–9868. [PubMed: 9275217]
41. Sohal RS, Allen RG, Farmer KJ, Newton RK. Iron induces oxidative stress and may alter the rate of aging in the housefly, *Musca domestica*. Mech Ageing Dev. 1985; 32:33–38. [PubMed: 3835414]
42. Sugarman B, Munro HN. Altered accumulation of zinc by aging human fibroblasts in culture. Life Sci. 1980; 26:915–920. [PubMed: 6990146]
43. Sullivan JL. Stored iron and ischemic heart disease. Empirical support for a new paradigm. Circulation. 1992; 86:1036–1037. [PubMed: 1516175]
44. Taketani S, Adachi Y, Nakahashi Y. Regulation of the expression of human ferrochelatase by intracellular iron levels. Eur J Biochem. 2000; 267:4685–4692. [PubMed: 10903501]
45. Walter, PB.; Beckman, KB.; Ames, BN. The role of iron and mitochondria in aging. In: Cadenas, E.; Packer, L., editors. Understanding the Process of Aging. New York: Marcel Dekker, Inc; 1999. p. 203-227.
46. Walter PB, Knutson MD, Paler-Martinez A, Lee S, Xu Y, Viteri FE, Ames BN. Iron deficiency and iron excess damage mitochondria and mitochondrial DNA in rats. Proc Natl Acad Sci U S A. 2002; 99:2264–2269. [PubMed: 11854522]
47. Wolf FI, Torsello A, Covacci V, Fasanella S, Montanari M, Boninsegna A, Cittadini A. Oxidative DNA damage as a marker of aging in WI-38 human fibroblasts. Exp Gerontol. 2002; 37:647–656. [PubMed: 11909682]
48. Yantiri F, Andersen JK. The role of iron in Parkinson disease and 1-methyl-4-phenyl-1,2,3,6-tetrahydropyridine toxicity. IUBMB Life. 1999; 48:139–141. [PubMed: 10794588]
49. Yip, R.; Dallman, PR. Iron. In: Ziegler, EE.; Filer, LJ., editors. Present Knowledge in Nutrition. Washington, DC: ILSI Press; 1996. p. 277-292.
50. Youdim MB, Riederer P. The role of iron in senescence of dopaminergic neurons in Parkinson's disease. J Neural Transm Suppl. 1993; 40:57–67. [PubMed: 8294901]

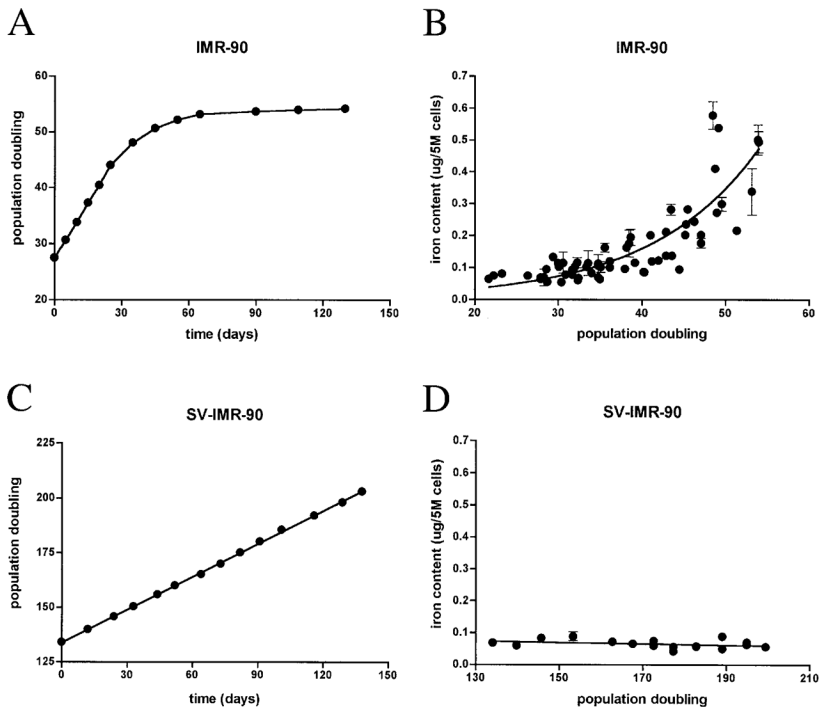

FIG. 1. IMR-90s accumulate iron during cellular senescence *in vitro*

(**A**) IMR-90 populations lose replicative capacity over time. Representative growth curve shows change in PD as a function of time, with senescence at 50–55 PD. Curve was fit by point-to-point function. (**B**) Increased total intracellular iron content as a function of PD in IMR-90s. Mean ± SD of iron content from $n = 20$ independent experiments was normalized to cell number (5×10^6 cells) and fit to an exponential function. Change in iron content during cellular senescence was ~10-fold, with doubling of iron content at every 8.9 PD. (**C**) In contrast, SV-IMR-90 populations do not lose replicative capacity over time in culture. Representative growth curve shows PD as function of time. Data were fit to a linear function ($r^2 = 0.9996$). (**D**) No change in total intracellular iron content detected as a function of PD in SV-IMR-90s. Mean ± SD from $n = 3$ independent experiments was normalized to cell number (5×10^6 cells) and fit to a linear function; slope was not significantly different from zero.

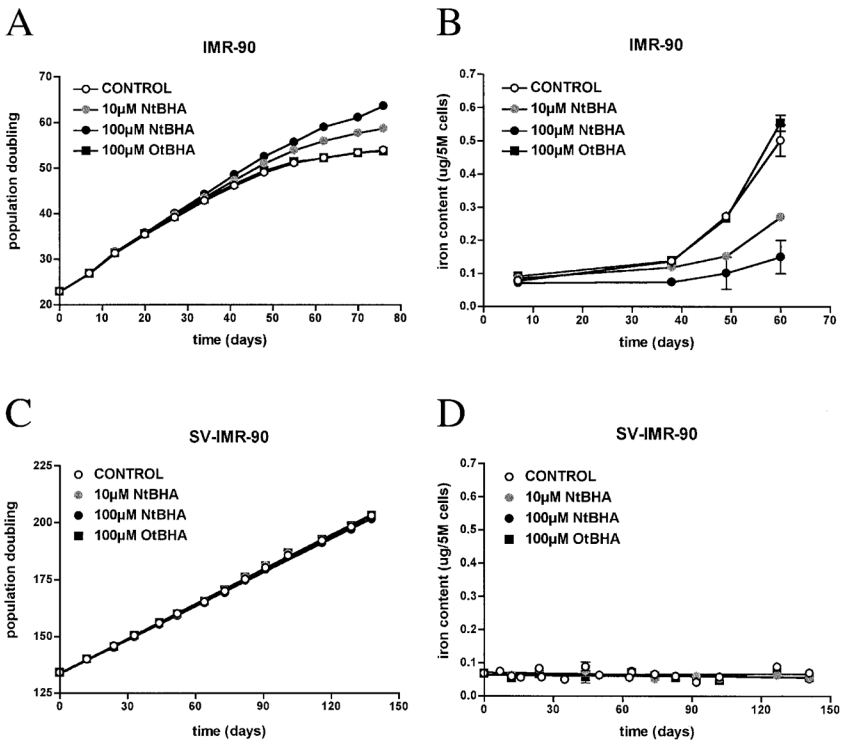

FIG. 2. NtBHA attenuates iron accumulation in IMR-90s during cellular senescence *in vitro*

IMR-90s were treated weekly with 10 μ*M* NtBHA (shaded circle), 100 μ*M* NtBHA (solid circle), or 100 μ*M* OtBHA (solid square). Representative growth curves (**A**) and total intracellular iron content (**B**) are shown. Curves were fit by point-to-point function. SV-IMR-90s were also treated weekly with 10 μ*M* NtBHA (shaded circle), 100 μ*M* NtBHA (solid circle), or 100 μ*M* OtBHA (solid square). Representative growth curves (**C**) and total intracellular iron content (**D**) are shown. Curves were fit to a linear function; no significance difference in growth or iron content was detected between treatments. Slopes of curves for iron content were not significantly different from zero.

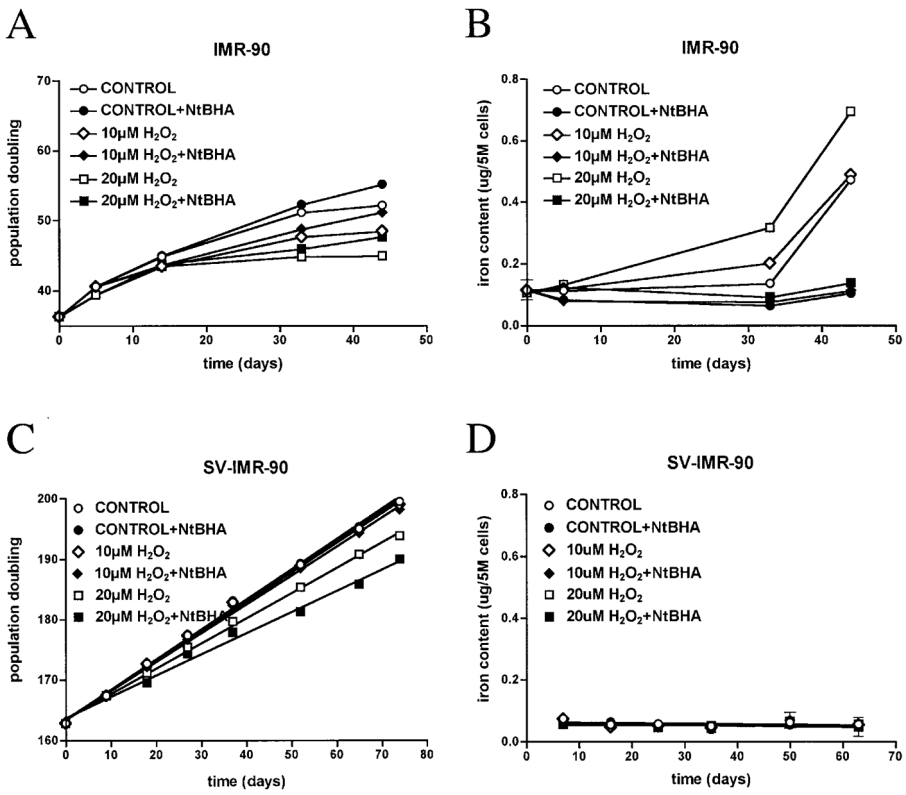

FIG. 3. H_2O_2 accelerates iron accumulation in IMR-90s during cellular senescence *in vitro*

IMR-90s were treated weekly with 10 μ*M* (diamonds) or 20 μ*M* H_2O_2 (squares). Twenty-four hours later, cultures were treated with (solid symbols) or without (open symbols) 100 μ*M* NtBHA. Representative growth curves (**A**) and total intracellular iron content (**B**) are shown. Curves were fit by point-to-point function. SV-IMR-90s were also treated weekly with 10 μ*M* (diamonds) or 200 μ*M* H_2O_2 (squares). Twenty-four hours later, cultures were treated with (solid symbols) or without (open symbols) 100 μ*M* NtBHA. Representative growth curves (**C**) and total intracellular iron content (**D**) are shown. Curves were fit to a linear function ($r^2 > 0.99$ for growth curves). Growth rates decreased with increasing H_2O_2; slopes of 20 μ*M* H_2O_2 ± NtBHA were significantly different from control. However, no difference in iron content was detected between treatments. Slopes of curves for iron content were not significantly different from zero.

Table 1

Total Metal Content in Human Cell Types as a Function of Cellular Senescence

	Average metal content (μg/5 × 10^6 cells)			
	Young	**Old**	**Doubling time of metal content (PD)**	**Fold change in metal content**
IMR-90				
Fe	0.050	0.511	8.9	10.2
K	29.055	92.692	17.9	3.2
Mg	1.463	7.923	12.3	5.4
Mn	0.006	0.013	29.3	2.0
Zn	0.176	0.725	14.7	5.4
HUVEC				
Fe	0.027	1.361	4.4	50.2
K	71.858	271.765	13.0	3.8
Mg	2.786	11.604	12.2	4.2
Mn	0.005	0.023	10.9	4.9
Zn	0.237	1.999	8.1	8.4
SV-IMR-90				
Fe	0.066	0.068	—	1.0
K	65.503	72.428	—	1.1
Mg	2.014	1.941	—	1.0
Mn	0.004	0.003	—	0.8
Zn	0.319	0.298	—	0.9

Average metal content was determined from data fit to exponential curve (IMR-90 and HUVEC) or linear curve (SV-IMR-90). Doubling time was determined from exponential curve as 0.69/rate constant (*K*). For IMR-90, “young” is 25 PD and “old” is 55 PD. For HUVEC, “young” is 35 PD and “old” is 60 PD. SV-IMR-90 values are shown for comparison although the populations do not senesce; “young” is 120 PD and “old” is 200 PD. Slopes of curves for all metals determined in SV-IMR-90 were not significantly different from zero, so no doubling time was calculated.

Table 2

Change in Metal Content in Human Cell Types as a Function of NtBHA or OtBHA Treatment

	Fold change in average metal content			
	Control	**10 μ*M* NtBHA**	**100 μ*M* NtBHA**	**100 μ*M* OtBHA**
IMR-90				
Fe	6.8	3.2	1.4	6.1
Mg	3.5	2.2	1.1	4.3
Zn	3.5	2.7	1.1	3.6
SV-IMR-90				
Fe	1.2	0.9	0.8	1.0
Mg	1.0	1.0	1.0	0.9
Zn	0.8	0.7	0.7	0.7

Fold change in average metal content was calculated as old metal content/young metal content. IMR-90 was cultured from PD 24 (“young”) to PD 51 (“old”) for control cells and SV-IMR-90 was cultured from PD 138 (“young”) to PD 190 (“old”) for control cells. Control values differ from those in Table 1 because cells were treated over a shorter span. IMR-90 data were fit to exponential curves and SV-IMR-90 fit to linear curves. Slopes for all conditions with each metal in SV-IMR-90 were not significantly different from each other. Potassium and manganese levels were not determined.

Table 3

Change in Metal Content in Human Cell Types as a Function of H_2O_2 ± NtBHA Treatment

	Fold change in average metal content					
	No NtBHA			100 μ*M* NtBHA		
	Control	10 μ*M* H_2O_2	20 μ*M* H_2O_2	Control	10 μ*M* H_2O_2	20 μ*M* H_2O_2
IMR-90						
Fe	4.5	4.6	6.6	1.0	1.1	1.3
Mg	3.2	3.4	2.2	1.4	1.2	1.0
Zn	2.4	2.6	1.6	1.2	1.0	0.8
SV-IMR-90						
Fe	1.0	0.9	1.0	0.9	1.0	0.8
Mg	0.8	0.8	1.2	0.8	1.0	1.1
Zn	0.6	0.6	0.9	0.6	0.7	0.9

Fold change in average metal content was calculated as old metal content/young metal content. IMR-90 was cultured from PD 36 (“young”) to PD 51 (“old”) and SV-IMR-90 was cultured from PD 162 (“young”) to PD 200 (“old”) for control cells. Control values differ from those in Table 1 because cells were treated over a shorter span. IMR-90 data were fit to exponential curves and SV-IMR-90 fit to linear curves. Slopes for all conditions with each metal in SV-IMR-90 were not significantly different from each other. Potassium and manganese levels were not determined.